Plasmonics (2014) 9:1091–1102
DOI 10.1007/s11468-014-9719-y

Generation of Multiple Fano Resonances in Plasmonic Split Nanoring Dimer

Adnan Daud Khan · Sultan Daud Khan · RehanUllah Khan · Naveed Ahmad · Amjad Ali · Akhtar Khalil · Farman Ali Khan

Received: 17 February 2014 / Accepted: 31 March 2014 / Published online: 11 April 2014

Abstract We present a computational study of the plasmonic response of a split nanoring dimer resonator which supports multiple plasmonic Fano-like resonances that arises by the coupling and interference of the dimer plasmon modes. For the generation of Fano resonances with large modulation depths, numerous configurations of the dimer resonator are analyzed which are observed to be highly dependent on the polarization of incident light. Moreover, the influence of dimension of the split nanoring structure on the spectral positions and intensities of the higher order Fano resonances are also investigated, and it is found that the asymmetric Fano line shapes can be flexibly tuned in the spectrum by varying various geometrical parameters. Such Fano resonators are also discovered to offer high values of figure of merit and contrast ratio due to which they are suitable for high-performance biological sensors.

Keywords Fano resonance · Plasmons · Split nanoring · Dimer · Figure of merit

A. D. Khan (✉) · R. Khan · A. Ali
Department of Electrical Engineering, Sarhad University of Science and Information Technology, LandiAakhun Ahmad, Ring road, 25000 Peshawar, Pakistan
e-mail: adnandaudkhan@gmail.com

R. Khan
e-mail: rehanmarwat1@gmail.com

A. Ali
e-mail: amjadalikhalil@gmail.com

S. D. Khan
Department of Information, Systems and Communication, University of Milan-Bicocca Piazza dell'Ateneo Nuovo, 1-20126 Milan, Italy
e-mail: sultan.khan@disco.unimib.it

N. Ahmad
Department of Chemical and Materials Engineering, Northern Borders University, Arar 1321, Saudi Arabia
e-mail: mscchemical@gmail.com

A. Khalil
Department of Electrical Engineering, University of Engineering and Technology, University road, 25000 Peshawar, Pakistan
e-mail: akhtarhussain83@hotmail.com

F. A. Khan
Department of Computer Science, COMSATS Institute of Information Technology, Kamra Road, Attock City 43600, Punjab, Pakistan
e-mail: farman_marwat@ciit-attock.edu.pk

Abbreviations

EIT	Electromagnetic-induced transparency
SERS	Surface-enhanced Raman spectroscopy
SRD	Split nanoring dimer
ISR	Isolated split nanoring
PIT	Plasmon-induced transparency
NRD	Nanoring dimer
Q	Quadrupole mode
O_1	First octupole mode
O_2	Second octupole mode
DQ	Dipole-quadrupole mode
QH	Quadrupole-hexadecapole mode
OH	Octupole-hexadecapolar mode
FoM	Figure of merit
CR	Contrast ratio
BW	Bandwidth
FWHM	Full width at half maximum
RIU	Refractive index unit

Introduction

Fano resonance in nanoscale plasmonic nanostructures arises from the interference of superradiant bright and subradiant

dark plasmon modes which are typically more sensitive to the geometry of the nanoparticles and changes in the refractive index (n) of the local environment [1]. The dipole moment of the bright mode is finite and can couple directly to the incident field due to which its spectral width broadened because of radiative damping. On the other hand, the dipole moment of the dark mode is extremely small (≈0) and cannot couple well to the incident field resulting in a narrow spectral width. By carefully designing the nanostructures, the broad superradiant and narrow subradiant plasmon modes can overlap, giving rise to strong asymmetric Fano line shape which is analogous to electromagnetic-induced transparency (EIT) observed in atomic system [2].

Various plasmonic nanostructures are analyzed over the past few years to study the effect of Fano resonances including nanoshells [3–5], ring/disk nanocavities [6–8], split rings [9, 10], disk with a missing wedge [11], nanocross [12], theta-shaped ring-rod [13], dimers [14–16], trimers [17], and nanoparticle chains [18]. Among all the structures, the plasmonic dimer nanoparticle has received a lot of attention due their controllably tunable plasmon resonances over the entire visible spectrum as well as near to mid-infrared region. The strong electromagnetic hot-spot produced in the gap regions of the nanodimer is essentially significant for surface-enhanced Raman spectroscopy (SERS) applications [19]. Numerous geometries based on dimer nanostructures are suggested to attain Fano resonances. Shao et al., have investigated the plasmonic dimer nanostructure based on a gold nanorod and a small gold nanosphere both theoretically and experimentally [20]. They achieved a single Fano resonance by locating the small nanosphere at different positions on the nanorod surface. Wu et al., have reported Fano-like resonances in the absorption spectrum of an asymmetric nanodimer of gold elliptical nanowires, which arises from the coherent coupling between the superradiant bright mode and the subradiant dark mode [21]. Yang et al. have demonstrated metallic nanorod dimers, where they examined a Fano resonance crop up by the interference between bright dipole mode of the short nanorod and dark quadrupole mode (Q) of the long nanorod [22]. Wu et al. have proposed a symmetry broken gold nanotube dimer and observed twined Fano-like resonances in the scattering spectrum [23]. However, the second Fano resonance obtained at the high energy level suffered from weak modulation depth. Khan and Miano studied a dimer based on mismatched gold nanocones and achieved single plasmonic Fano resonance that emerges from the coupling of bright dipole and dark quadrupole modes [14]. Recently, Khan et al., have investigated a dimer nanostructure based on symmetric and asymmetric multilayered nanoshell dimer where multiple Fano resonances are achieved in the asymmetric nanodimer [15]. The problem with the reported dimer nanostructures is that either the Fano resonances suffer from weak modulation depths or the fabrication of such nanostructures are quite complex which demand the use of open structures.

We present here a very simple plasmonic dimer nanostructure constructed from split nanorings and attained multiple Fano resonances in the extinction spectra. Several research groups have fabricated [9, 24] and studied the split nanoring structures for various applications including metamaterials [25], sensing [26], slow light, and EIT [27]. We demonstrated various arrangements of the dimer nanostructure with special emphasis on the Fano asymmetric line shape. All the configurations are found to be highly dependent on the polarization of the incident field due to which distinct Fano resonances are obtained for both the longitudinal and transverse polarizations. The hybridized modes and Fano dips can be flexibly tuned in the spectrum by modifying the geometric parameters. The higher-order multiple Fano resonances with large modulation depths obtained in our proposed nanostructure present clear advantages over the heptamer clusters composed of several split nanorings, as our structures reduce the overhead due to fabrication complexity related to heptamer clusters or nanoparticle aggregate architectures. Eventually, we calculated the figure of merit (FoM) and contrast ratio (CR) by changing the refractive index of the dielectric medium. Both the high contrast ratio and high figure of merit make the dimer resonator suitable for chemical and biological sensing.

Structure and Numerical Model

The schematic of the split nanoring dimer (SRD) resonator is illustrated in Fig. 1. The SRD consists of two metallic gold (Au) nanorings with twin gaps, where the thickness of the Au layer is W, the width is H, the distance between the two gaps is G, the length between the two split nanorings is D, and the outer radius is R. The incident light is a time harmonic linearly polarized plane wave. The electric field is directed along y-axis and the wave propagates in the x-direction. The optical properties of the nanoparticles are analyzed using two values of the rotation angle θ i.e., θ=0° and 90°. We define the dimer axis along x-axis. For θ=0°, the incident light is polarized perpendicular and the propagation direction is along the dimer axis, while for θ=90°, the polarization is parallel and the propagation direction is perpendicular to the dimer axis. Throughout the paper, the values for W, H, G, and R are fixed at 30, 20, 30, and 75 nm, respectively. The minimum value of D for SRD is chosen to be 2 nm to omit the quantum mechanical effects that amend the classical response [14, 15]. All the simulations have been carried out by COMSOL with RF module. The experimentally measured Johnson and Christy data have been utilized for the dielectric constant of the gold [28]. The embedding medium is considered air for all the cases.

Results and Discussion

Single Split Nanoring

We start our discussion from an isolated split nanoring (ISR) and analyzed its optical extinction properties for two values of the rotation angle θ i.e., θ=0° and 90° as shown in Fig. 2. The blue curve corresponds to longitudinal excitation, where the resonant plasmon peak near 1.46 eV shows a superradiant dipole mode and the peak around 1.17 eV shows a subradiant quadrupole mode. The nature of the modes is also revealed by the surface charge distributions shown in the inset where the broad peak displays a bright dipolar pattern (mode oscillation in phase), while the narrow peak exhibits a dark quadrupolar pattern (mode oscillation out of phase). Because of the small energy gap, the two resonant modes overlap and induce a Fano resonance in the spectrum with a dip around 1.27 eV. This Fano resonance can be considered as plasmon-induced transparency (PIT), which is envisaged and examined in metamaterials [2, 29, 27]. The red curve corresponds to transverse polarization, where the lower order dipole mode disappears and the higher order quadrupole mode at 1.89 eV and octupole mode at 1.22 eV emerge in the spectrum. However, there is a large energy gap between the two modes due to which they will not interact with each other as a result; no Fano resonance is observed in this case. This phenomenon indicates that by adjusting the polarization of incident light, the Fano resonance can be switched on and off like in the conventional nanodimers [14, 30, 22, 16]. The results of the simulations are consistent with similar theoretical results reported for plasmonic heptamer clusters composed of split nanorings [10].

Split Nanoring Dimer (SRD)

Next, we construct a nanodimer resonator consisting of two split nanorings with a separation of 2 nm. Numerous configurations of the dimer resonator are analyzed as demonstrated in Fig. 3 to study the effect of Fano resonances.

Model I SRD

In this configuration, the split nanorings are arrange in such a way that the openings (gap (G)=30 nm) of the two rings are in the vertical direction (along y-axis) as shown in Fig. 3a. Figure 4a shows the extinction spectra of model I resonator for θ=0° and 90°. The resonant extinction peaks arises by the strong interactions of the hybridized modes of the two split nanorings. For the blue curve, we observed the similar modes and Fano resonance as in ISR. This is also revealed by the induced surface charge distributions shown in the inset, where the mode around 1.40 eV shows a bright dipolar mode because both the nanoparticles display a dipolar pattern, while the hybridized mode near 1.2 eV shows a dark quadrupolar mode as both the nanoparticles display a quadrupolar pattern. However, the extinction intensities of the modes in this case are greater than ISR because these modes arise from the strong coupling of two split nanorings. For θ=90° (red curve), we obtained three resonant extinction peaks in the spectrum where the peaks around 1.60 and 2.00 eV shows the hybridized octupole (O_1 and O_2) modes, while the peak near 1.20 eV shows a hybridized quadrupole (Q) mode. All the hybridized modes have the similar nature as that of ISR for θ=90°. However, in this case, a pronounced Fano resonance is observed near 1.85 eV which was absent in ISR. So in model I resonator, we obtained distinct plasmonic Fano-like resonances for both the transverse and longitudinal polarizations.

Figure 4b shows the distribution of the electric field of model I nanodimer which is calculated at each resonant peak for both the values of θ. The strong fields are concentrated both in the gap region (G) and at the interparticle distance (D) of the dimer. For θ=0°, the maximum value of the intensity enhancement for the dipole mode is 86 while that of the quadrupole mode is 71. For θ=90°, the maximum value of the field enhancement for the O_2 mode is observed to be 61 while that for the Q mode is 50. The highest value is found for the O_1 mode which is approximately 295. The reason for the highest values obtained in case of 90° is because the electric field is aligned with the dimer axis which will allows more light to concentrate in the narrow gap regions. Such values of the intensity enhancement are typically suitable for the SERS applications by detecting biomolecules [19, 31].

Since the model I resonator provides Fano resonance, so in the following, we will show that by varying the geometrical

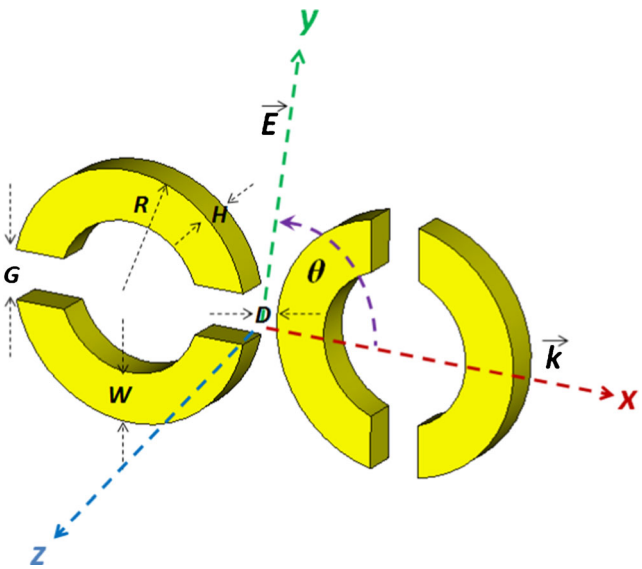

Fig 1 Schematic illustration of split nanoring dimer. The geometry parameters W, H, G, R, and D are 30, 20, 30, 75, and 2 nm, respectively. The incident light is polarized along y-axis and the wave propagates along x-axis

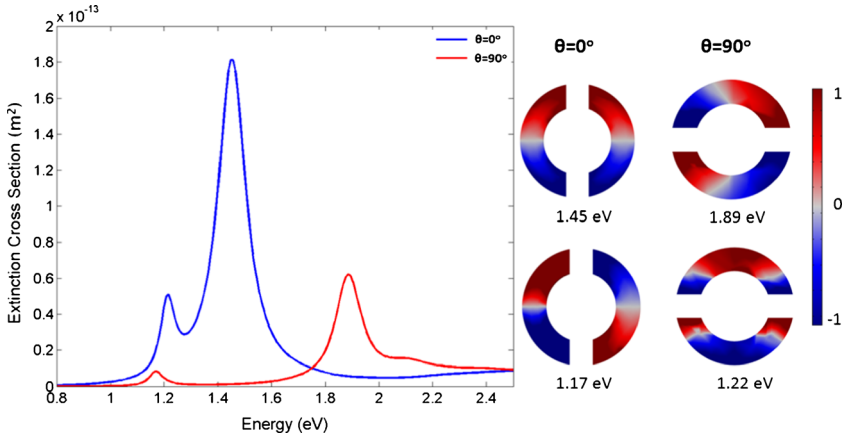

Fig 2 Extinction spectra of ISR for two values of the rotation angle θ i.e., θ=0° and 90°. Inset shows surface charge distributions corresponding to each peak in the extinction spectrum

parameters, there is a large tunability of the hybridized modes and Fano resonances. Figure 5a shows the extinction spectra as a function of size (R) of model I SRD. It is observed that by increasing R, the broad O_1 mode slightly shift to lower energy level (red-shift) and its spectral width increases. However, the O_2 mode near 2.00 eV and the Q mode near 1.20 eV have somewhat sustain their spectral positions which can also be seen in Fig. 5b. For low values of R, the Fano resonance is observed at the high energy shoulder of the broad mode near 1.85 eV, but as R increases, the Fano resonance switches to low energy shoulder of the broad mode near 1.25 eV (at R=105 nm). So, the Fano resonance can be switched from higher to lower energy values in the spectrum and vice versa by varying R.

Figure 6 presents the dependence of the hybridized plasmon modes on the gap region (G) at fixed D=2 nm. At G= 0 nm, the SRD adopts the shape of the nanoring dimer (NRD) where the broad peak at the lower energy level near 1.10 eV represents the superradiant dipole plasmon mode and a slight peak at the high energy level near 1.91 eV shows a subradiant quadrupole plasmon mode. Such modes have also been found in the conventional nanodimers [32, 33, 14]. However, as we increase the value of G (splitting NRD), the nature of the hybridized modes strongly changes and a new mode appears around 0.96 eV as shown by the green curve. The nature of these modes is discussed in Fig. 4. It also appears that there is a simultaneous blue-shift of the plasmonic modes as the value of G increases and the spectral separation between the modes decreases as shown in Fig. 6b where the O_1 and O_2 modes presents greater shift towards blue. For model I resonator, modifying G, produces only single weak Fano resonance near 1.85 eV (G=40 nm).

Figure 7 shows the extinction spectra of model I resonator as a function of the interparticle distance (D). The broad O_1 mode strongly blue-shifts, while the O_2 mode near 2.00 eV disappears and as we increase D. The increase in D also vanishes the Fano resonance; however, the Q mode near 1.20 eV is examined to be independent of the values of D.

Figure 8 shows the extinction spectra of model I resonator obtained by modifying the width (H). It is observed that increasing the value of H results in a blue-shift of the plasmonic peaks and their spectral width increases. Moreover, the Fano resonance at the higher energy shoulder of the broad mode also disappears because the O_2 mode vanishes as in the case of varying D. On the lower energy side, by increasing H, the Q mode gained strength, becomes slightly broad, and also the separation between the Q mode and O_1 mode decreases. Due to the near-field coupling between the two modes, a Fano resonance with sharp modulation depth is induced in the spectrum (H=80 nm). So, similar to parameter R, changing H can also switch the Fano resonance

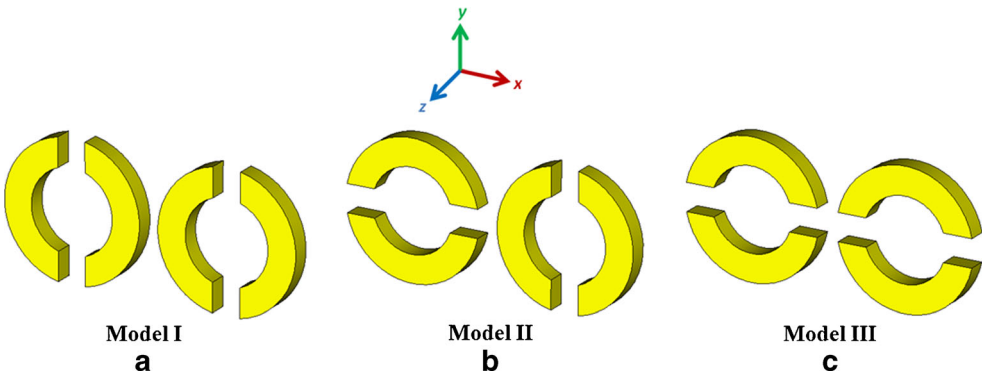

Fig 3 Schematics of various split nanoring dimer plasmonic nanostructures

from higher to lower energy values in the spectrum and vice versa.

Model II SRD

In this configuration, the split nanorings are arrange in such a way that the openings (gap (G)=30 nm) of the two rings are perpendicular to each other as shown in Fig. 3b. Figure 9a shows the extinction spectra of model II resonator for two different polarizations. For θ=0° (blue curve), we obtained four hybridized modes and multiple Fano resonances in the spectrum due to strong capacitive coupling (near-field interaction). The fundamental Fano dip around 1.30 eV is almost at the same spectral location as that of the ISR's Fano

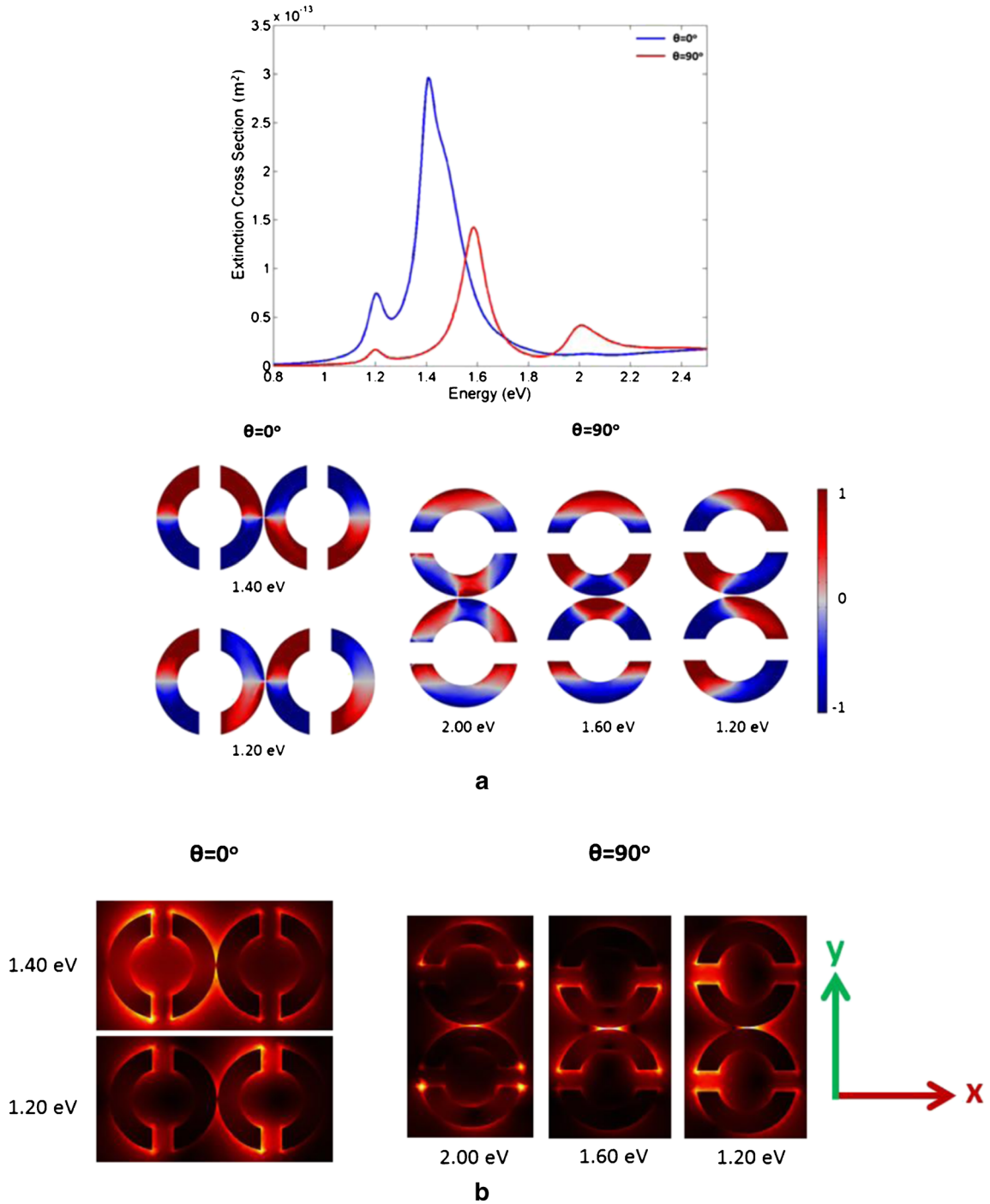

Fig 4 **a** Extinction spectra of model I nanodimer for two values of θ i.e., θ=0° and 90°. Inset below shows surface charge distributions corresponding to each peak in the extinction spectrum. **b** Distributions of the real part of the electric field in the xy-plane (z=0) of model I nanodimer for each resonant peak

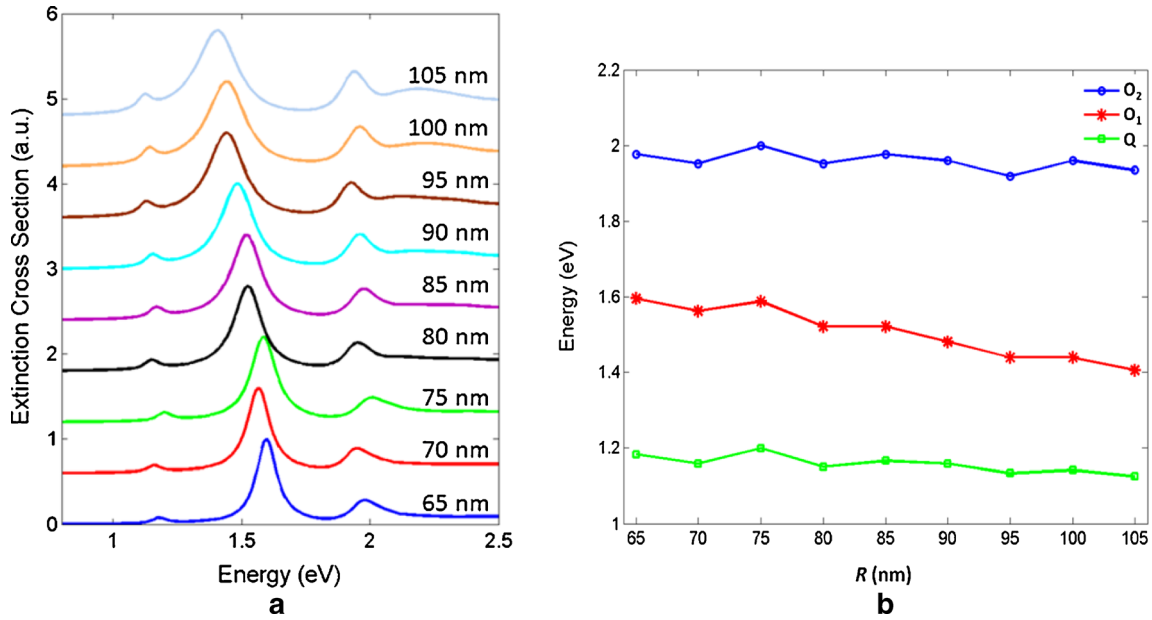

Fig 5 **a** Extinction spectra of model I nanodimer for different values of *R*. **b** Energy shift as a function of *R*

dip. By observing the induced surface charge distributions, the broad resonant mode around 1.46 eV represent a quadrupole distribution on the first nanoparticle and a dipole distribution on the second one. Thus, this mode is a combination of dipole and quadrupole modes (DQ). This mode was originally dipolar in nature as in ISR and in model I resonator, but in this configuration, its nature is changed because of the strong hybridization between the two nanoparticles. The peak near 1.22 eV displays a quadrupolar pattern on the first nanoparticle and a hexadecapolar pattern on the second one. So, this hybridize mode represents a mix quadrupole-hexadecapole (QH) mode. The nature of QH mode is also highly changed like the DQ mode. This mode was quadrupolar in character in the previous arrangements, but here at the narrow gap between the two nanorings, the transfer of the charges occurs i.e., the charges of the left nanoparticle migrate to the right one due to which the nature of this mode appears as hexadecapolar. The peak near 1.13 eV shows a quadrupolar pattern (Q) on both the nanoparticles, while the resonant mode near 1.91 eV displays an octupole distribution on the first nanoparticle and a hexadecapolar distribution on the second nanoparticle. So, this charge distribution clearly shows the mixed octupole-hexadecapolar character of the octupole-hexadecapolar (OH) mode. Thus, in model II configuration, we obtained three distinct plasmonic Fano-like resonances which arise by the coupling and interaction of the higher order hybridized modes

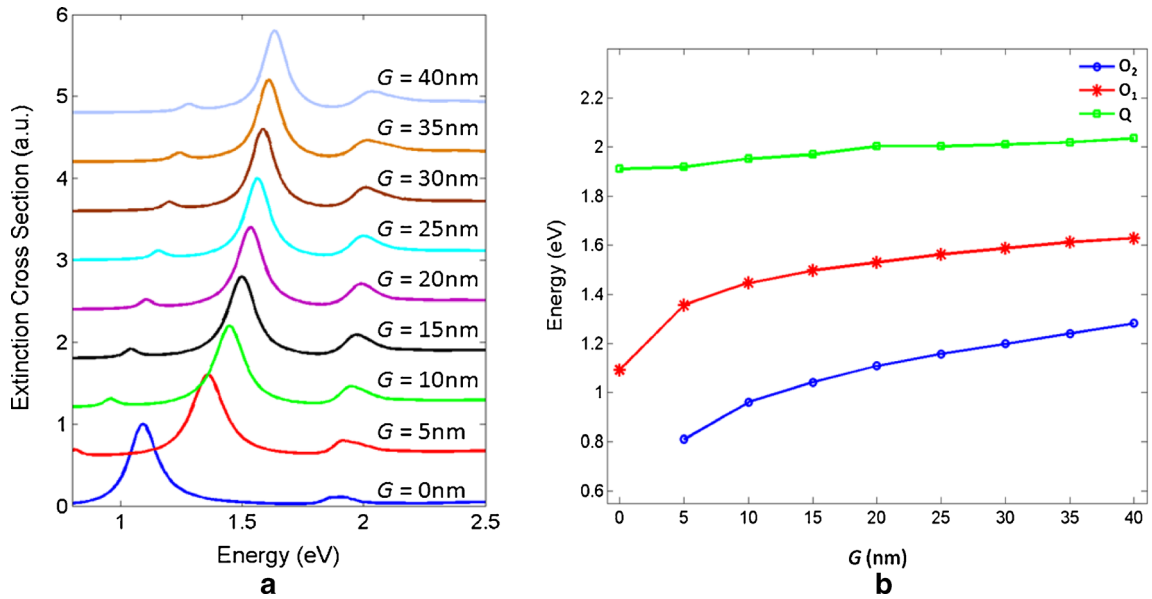

Fig 6 **a** Extinction spectra of model I nanodimer for different values of *G*. **b** Energy shift as a function of *G*

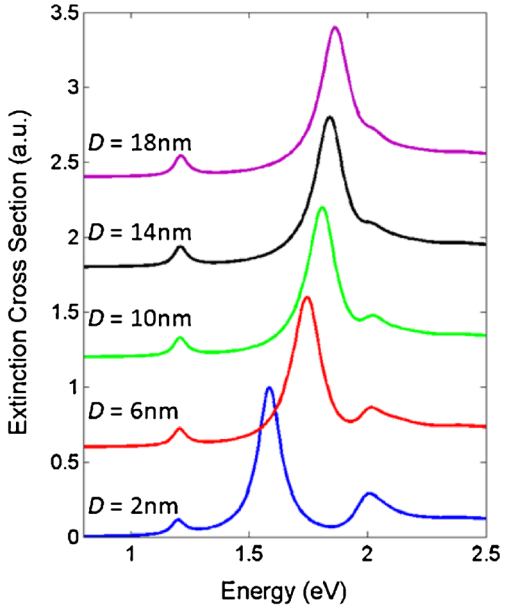

Fig 7 Extinction spectra of model I nanodimer for different values of D

with the broad DQ mode. These higher order multiple Fano resonances with large modulation depths can be used for multiwavelength SERS and plasmon line shaping by modifying the plasmon line at several locations simultaneously [10, 34]. Liu et al., have achieved multiple Fano resonances by constructing heptamer clusters using split nanoring structures [10]. However, we attained multiple Fano resonances using only two split nanorings (dimer). This will reduce the fabrication cost and complexity and can be used in a wider range of technological applications. Moreover, to our knowledge, these types of higher order multiple Fano resonances have never been reported before in any dimer nanostructure by using such a simple structure as nanoring. For θ=90° (red curve), we

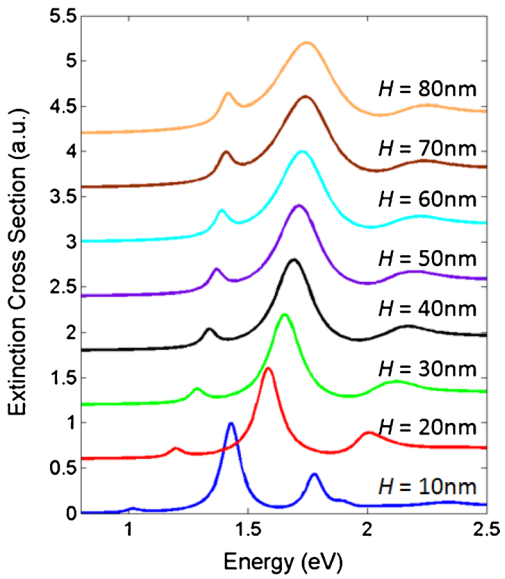

Fig 8 Extinction spectra of model I nanodimer for different values of H

obtained a single Fano resonance near 1.92 eV, which suffers from weak modulation depth. Thus, by changing θ or the polarization of incident light, we can obtain different plasmonic Fano-like resonances.

Figure 9b displays the electric field distributions of model II nanodimer which is calculated at each resonant peak for both the values of θ. For θ=0°, the highest values of the field enhancement for the DQ, Q, QH, and OH modes are 67, 78, 62, and 107, respectively. For θ=90°, the maximum value is found only for the dipole mode which is around 138. The transversely polarized incident light excites current along the whole SRD structure which results in a larger field in the gap regions compared to longitudinal polarization. So, the SRD nanostructure is capable of focusing more power from the transversely polarized incident beam. From the field enhancement values, it becomes clear that model II resonator is a better choice for both the multiwavelength SERS applications [29].

In the following, we show that by modifying the structural parameters of model II Fano resonator, there is a large tunability of the hybridized modes and Fano resonances. Figure 10 reveals the extinction spectra of model II SRD as a function of R. It seems that the increase in R slightly affects the spectral position of all the hybridized modes. Furthermore, the modulation depth of the Fano resonances and the dipole moment of the bright DQ mode near 1.46 eV also dramatically increase with an increase of R. The sharp Fano resonances with large modulation depths are observed at R=105 nm, which are located at both the high and low energy shoulder of the bright superradiant DQ mode. Thus, in model II resonator, modifying R will greatly affect the asymmetric Fano line shapes. Such Fano resonator is highly useful for plasmon line shaping and multiwavelength biosensing applications [34, 15].

Figure 11 shows the extinction spectra of model II Fano resonator which is obtained by modifying the gap (G). Again at G=0 nm, the model II SRD shaping like a NRD and the modes obtained are similar to that of model I NRD except that the broad dipole mode in this case is slightly blue-shifted. As the value of G increases, the nature of the modes changes and two higher-order hybridized modes start to appear at the lower energy shoulder of the broad mode. Also, with the increase of G, all the resonant modes simultaneously blue-shifted and the modulation depths of the Fano resonances increase. This shows the strong dependence of the Fano resonances and higher order dark modes on G.

Figure 12 represents the extinction spectra as a function of the interparticle distance (D). Unlike the previous cases, no broadening and shifting of the bright DQ mode are obtained by varying D. In fact, all the hybridized modes have maintained their spectral position by modifying D except the hybridized quadrupole mode near 1.13 eV (blue curve), blue-shifts and finally vanishes as D increases. So, large value of D results in the destruction of Fano resonances.

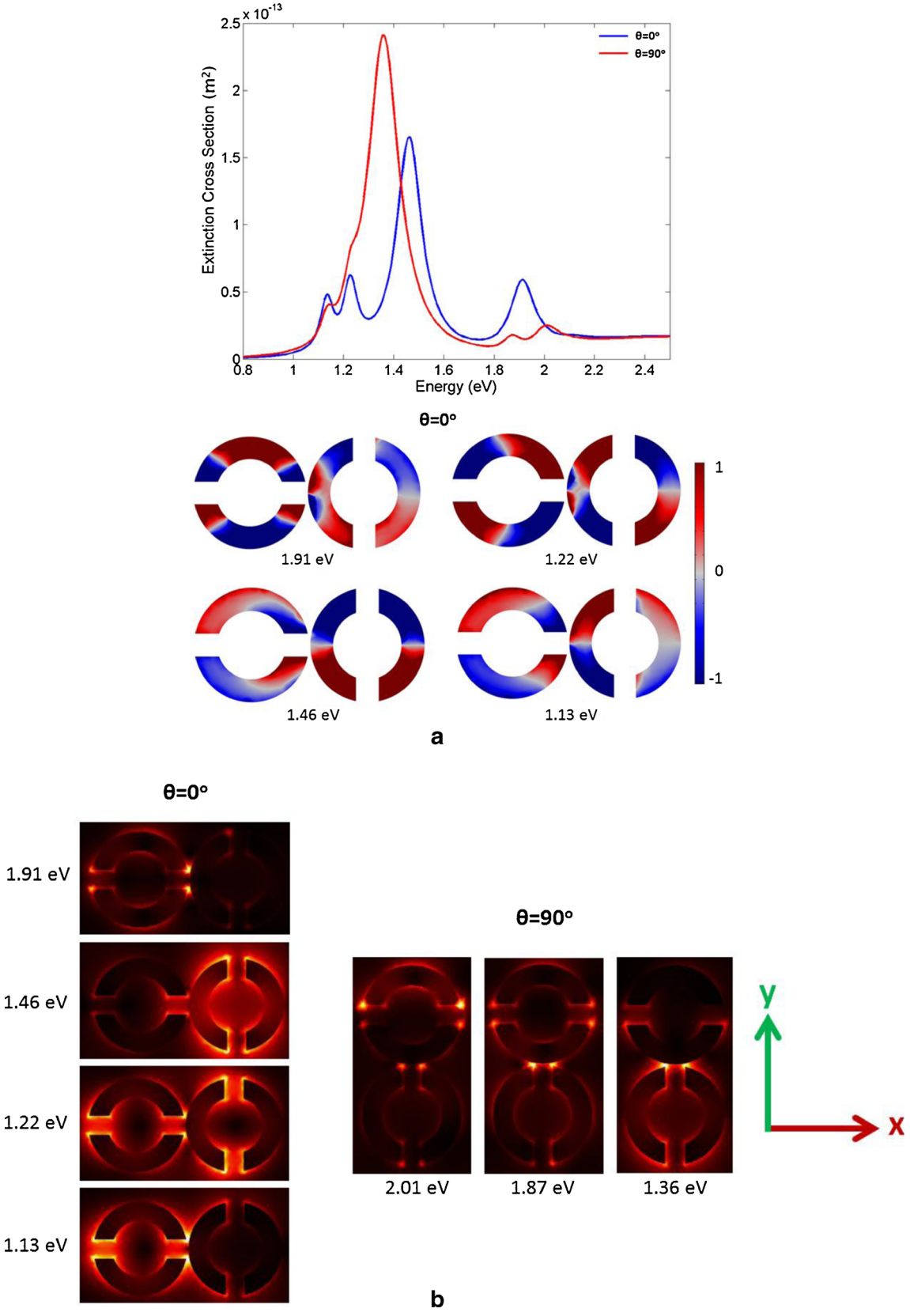

Fig 9 **a** Extinction spectra of model II nanodimer for two values of θ i.e., θ=0° and 90°. Inset below shows surface charge distributions corresponding to each peak in the extinction spectrum. **b** Distributions of the real part of the electric field in the *xy*-plane (z=0) of model II resonator for each resonant peak

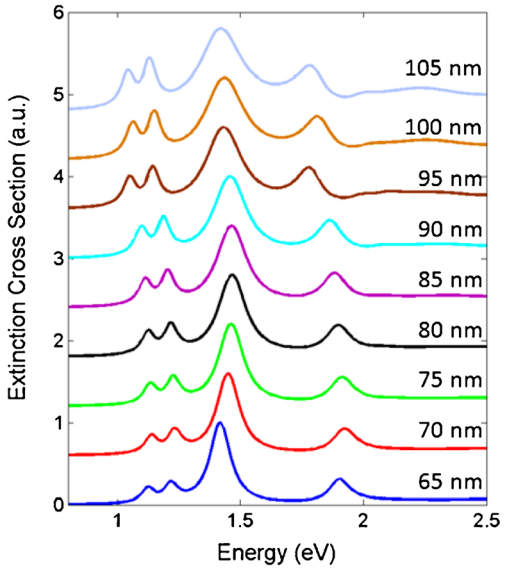

Fig 10 Extinction spectra of model II resonator for different values of *R*

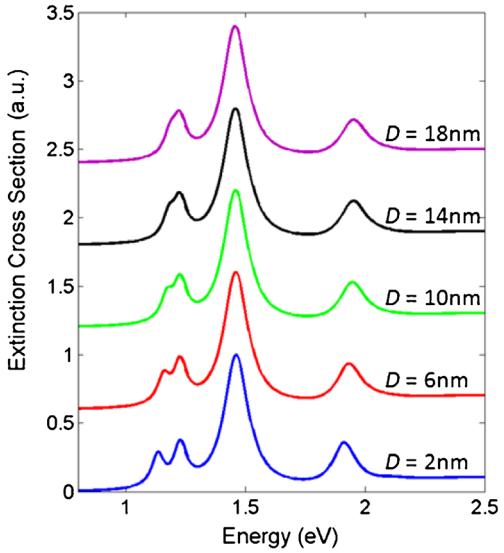

Fig 12 Extinction spectra of model II resonator for different values of *D*

Figure 13 shows the extinction spectra of model II nanodimer obtained by changing the width (*H*). It is found that the parameter *H* significantly affects the hybridized plasmonic modes. The bright DQ mode blue-shifts and widens, whereas the Q and QH modes at the lower energy side acquire sufficient strength at large values of *H*. Also, as *H* increases, the OH mode at the higher energy side loses its strength and finally disappears in the spectrum. So, for high values of *H*, the Fano resonance at the high energy shoulder of the broad mode vanishes, whereas, at the low energy shoulder, two sharp Fano resonances with large modulation depths are obtained.

Model III SRD

In this configuration, the split nanorings are arrange in such a way that the openings (gap (*G*)=30 nm) of the two rings are in the same direction as shown in Fig. 3c. Figure 14 shows the extinction spectra of model III resonator for the two different polarizations. In this model, the optical response changes drastically; only a single broad plasmonic peak is obtained in the spectrum for both the polarizations. Thus, model III SRD is not proficient for the Fano resonance generation.

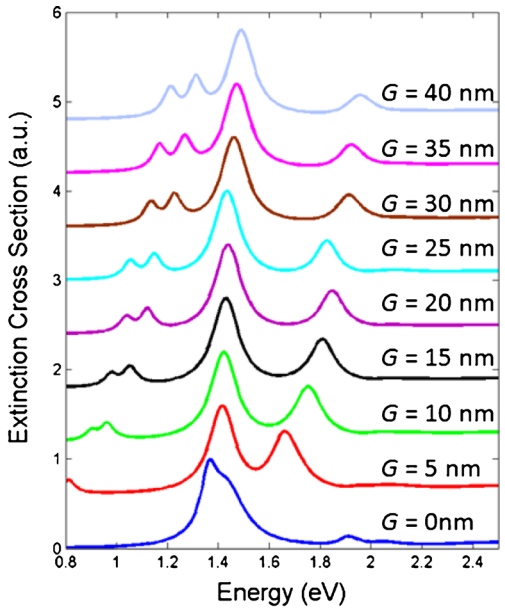

Fig 11 Extinction spectra of model II resonator for different values of *G*

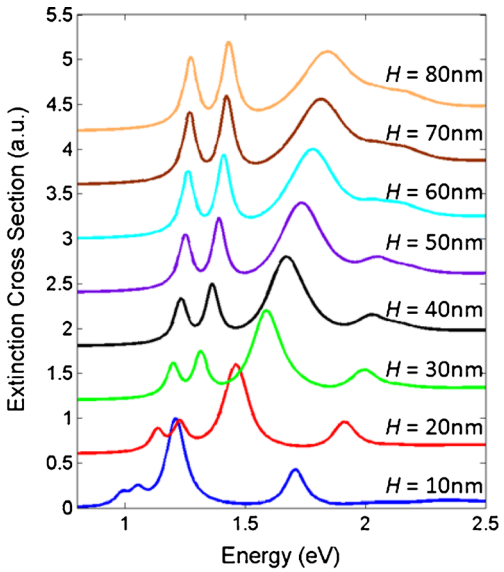

Fig 13 Extinction spectra of model II resonator for different values of *H*

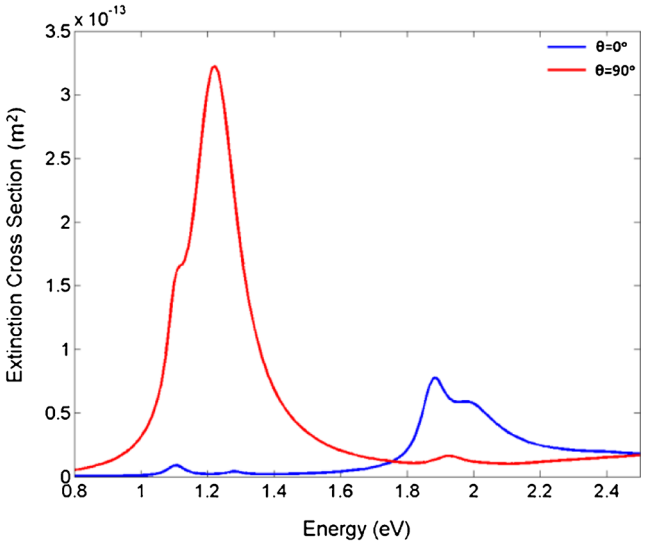

Fig 14 Extinction spectra of model III nanodimer for two values of θ i.e., θ=0° and 90°

Sensing with Nanodimer

Since the model II configuration is proved to provide multiple Fano resonances, so it can be used as broadband biosensor compared to other two models. The performance of the model II SRD as a biosensor is analyzed by using figure of merit (FoM) and contrast ratio (CR) which are obtained by changing the refractive index (n) of the local environment. The FoM is the ratio of the sensitivity to the bandwidth (BW) of the resonance plasmon mode as given by Eq. (1). The BW is usually obtained as the full width at half maximum (FWHM) for symmetric plasmon resonances; however, for asymmetric resonances, the BW is the line width from the peak to the dip of the resonance as suggested by Hao et al [35]. The contrast ratio is calculated by taking the difference of the peak (P) and dip (D) values over the sum of these two values as given by Eq. (3). Figure 15a presents the extinction spectra of model II SRD for different values of n. It appears that, increasing n results in a simultaneous red-shift of the hybridized plasmonic modes. Figure 15b exhibits the energy shifts of the resonant modes as a function of n. The sensitivity of the Q mode is 0.928 eV RIU^{-1}; the FoM and CR values are 5.1 and 60 %, respectively. The sensitivity of the bright DQ mode is 0.86 eV RIU^{-1}; the FoM and CR values are 8 and 70 %, respectively. The sensitivity of the QH mode is 0.7276 eV RIU^{-1}; the FoM and CR values are 10 and 35 %, respectively. The sensitivity of the OH mode is 0.678 eV RIU^{-1}; the FoM and CR values are 16.2 and 20 %, respectively. The values of the sensitivities, FoM, and CR obtained from our simple nanostructure are close to previously reported complex nanostructures [6, 36, 1], and these values also reveal the performance of the model II SRD as a biological sensor.

$$\text{FoM} = \left.\frac{\text{Sensitivity}}{\text{BW}}\right|_{n = 1.00} \tag{1}$$

$$\text{Sensitivity} = \frac{E_{\max}(n = 1.00) - E_{\max}(n = 1.50)}{n_{\max} - 1} \tag{2}$$

$$\text{CR} = \left.\frac{P - D}{P + D}\right|_{n = 1.00} \tag{3}$$

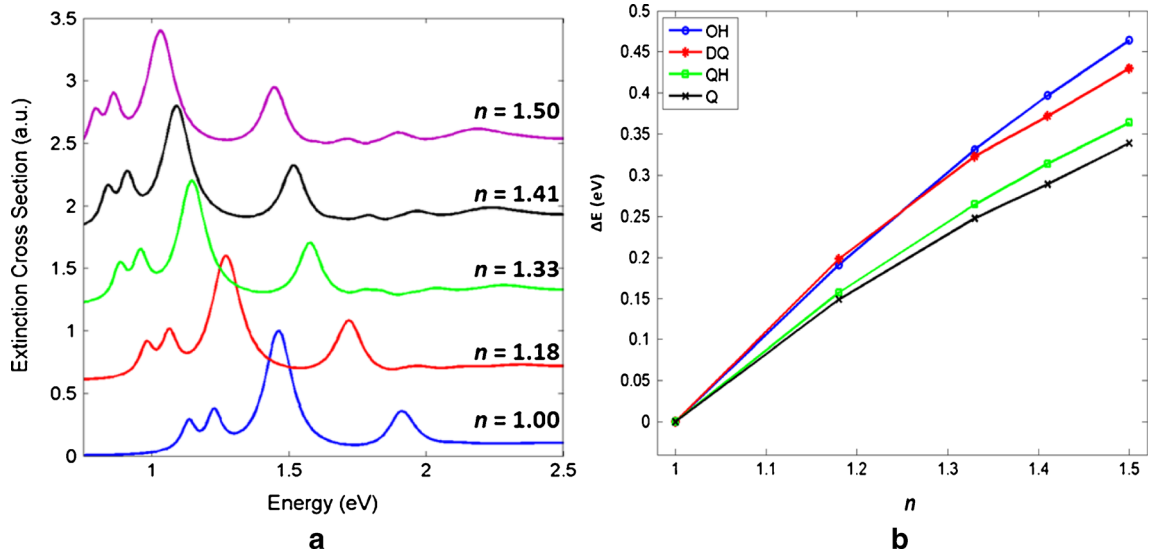

Fig 15 **a** Local refractive index sensitivity of model II nanodimer at θ=0°. The refractive index of the surrounding media is n=1.00, 1.18, 1.33, 1.41, and 1.50. **b** Energy shits of OH, DQ, QH, and Q modes as a function of n

Conclusion

We systematically investigated the generation and manipulation of higher order multiple Fano resonances in a nanodimer composed of split nanorings. The Fano resonances are induced when a multipolar resonance spectrally overlaps with a broad plasmon resonance. Various configurations are proposed to achieve unique and tunable Fano resonances at different frequencies for both the transverse and longitudinal polarizations. The modulation depth as well as the spectral position of the Fano resonances observed in all the nanostructures can be flexibly tuned in the spectrum by modifying the structure parameters. Among all the models, the model II resonator is discovered to provide higher-order multiple Fano resonances with large modulation depths that are highly suitable for plasmon line shaping and can serve as platforms for multiwavelength sensing applications. However, model I nanodimer exhibits high values of the field enhancement at various regions in the optical spectrum, which is greatly appropriate for SERS applications by detecting biomolecules. The spectral sensitivity of model II Fano resonator to the surrounding medium is also analyzed and high values of FoM and CR are obtained, which clearly reveals that the Fano resonator can be used for biological sensing. The generation of multiple plasmonic Fano resonances in our proposed design presents clear advantages over the complex nanostructures and nanoparticle aggregates as their fabrication are simpler and can be utilized in a larger range of technological applications.

References

1. Khan AD, Miano G (2013) Plasmonic fano resonances in single-layer gold conical nanoshells. Plasmonics 8(3):1429–1437
2. Chen J, Wang P, Chen C, Lu Y, Ming H, Zhan Q (2011) Plasmonic EIT-like switching in bright-dark-bright plasmon resonators. Opt Express 19(7):5970–5978
3. Khan AD, Miano G (2013) Higher order tunable Fano resonances in multilayer nanocones. Plasmonics 8(2):1023–1034
4. Mukherjee S, Sobhani H, Lassiter JB, Bardhan R, Nordlander P, Halas NJ (2010) Fanoshells: nanoparticles with built-in Fano resonances. Nano Lett 10(7):2694–2701
5. Peña-Rodríguez O, Rivera A, Campoy-Quiles M, Pal U (2013) Tunable Fano resonance in symmetric multilayered gold nanoshells. Nanoscale 5(1):209–216
6. Fu YH, Zhang JB, Yu YF, Luk'yanchuk B (2012) Generating and manipulating higher order Fano resonances in dual-disk ring plasmonic nanostructures. ACS Nano 6(6):5130–5137
7. Cetin AE, Altug H (2012) Fano resonant ring/disk plasmonic nanocavities on conducting substrates for advanced biosensing. ACS Nano 6(11):9989–9995
8. Zhang Y, Jia T, Zhang H, Xu Z (2012) Fano resonances in disk–ring plasmonic nanostructure: strong interaction between bright dipolar and dark multipolar mode. Opt Lett 37(23):4919–4921
9. Lahiri B, McMeekin SG, De La Rue RM, Johnson NP (2013) Enhanced Fano resonance of organic material films deposited on arrays of asymmetric split-ring resonators (A-SRRs). Opt Express 21(8):9343–9352
10. Liu S-D, Yang Z, Liu R-P, Li X-Y (2012) Multiple Fano resonances in plasmonic heptamer clusters composed of split nanorings. ACS Nano 6(7):6260–6271
11. Fang Z, Cai J, Yan Z, Nordlander P, Halas NJ, Zhu X (2011) Removing a wedge from a metallic nanodisk reveals a Fano resonance. Nano Lett 11(10):4475–4479
12. Verellen N, Van Dorpe P, Huang C, Lodewijks K, Vandenbosch GA, Lagae L, Moshchalkov VV (2011) Plasmon line shaping using nanocrosses for high sensitivity localized surface plasmon resonance sensing. Nano Lett 11(2):391–397
13. Habteyes TG, Dhuey S, Cabrini S, Schuck PJ, Leone SR (2011) Theta-shaped plasmonic nanostructures: bringing "dark" multipole plasmon resonances into action via conductive coupling. Nano Lett 11(4):1819–1825
14. Khan AD, Miano G (2013) Investigation of plasmonic resonances in mismatched gold nanocone dimers. Plasmonics 9(1):35–45
15. Khan AD, Khan SD, Khan RU, Ahmad N (2013) Excitation of multiple Fano-like resonances induced by higher order plasmon modes in three-layered bimetallic nanoshell dimer. Plasmonics. doi: 10.1007/s11468-013-9644-5
16. Xi Z, Lu Y, Yu W, Wang P, Ming H (2013) Improved sensitivity in a T-shaped nanodimer plasmonic sensor. J Opt 15(2):025004
17. Mei Z, Liang-Sheng L, Ning Z, Qing-Fan S (2013) The Fano-like resonance in self-assembled trimer clusters. Chin Phys Lett 30(7):077802
18. Wang M, Cao M, Chen X, Gu N (2011) Subradiant plasmon modes in multilayer metal–dielectric nanoshells. J Phys Chem C 115(43):20920–20925
19. Ye J, Wen F, Sobhani H, Lassiter JB, Dorpe PV, Nordlander P, Halas NJ (2012) Plasmonic nanoclusters: near field properties of the Fano resonance interrogated with SERS. Nano Lett 12(3):1660–1667
20. Shao L, Fang C, Chen H, Man YC, Wang J, Lin H-Q (2012) Distinct plasmonic manifestation on gold nanorods induced by the spatial perturbation of small gold nanospheres. Nano Lett 12(3):1424–1430
21. Wu D, Jiang S, Liu X (2012) Fano-like resonances in asymmetric homodimer of gold elliptical nanowires. J Phys Chem C 116(25):13745–13748
22. Yang Z-J, Zhang Z-S, Zhang L-H, Li Q-Q, Hao Z-H, Wang Q-Q (2011) Fano resonances in dipole-quadrupole plasmon coupling nanorod dimers. Opt Lett 36(9):1542–1544
23. Wu D, Jiang S, Cheng Y, Liu X (2012) Fano-like resonance in symmetry-broken gold nanotube dimer. Opt Express 20(24):26559–26567
24. Zhang Q, Wen X, Li G, Ruan Q, Wang J, Xiong Q (2013) Multiple magnetic mode-based Fano resonance in split-ring resonator/disk nanocavities. ACS Nano 7(12):11071–11078
25. Pryce IM, Aydin K, Kelaita YA, Briggs RM, Atwater HA (2010) Highly strained compliant optical metamaterials with large frequency tunability. Nano Lett 10(10):4222–4227
26. Lahiri B, Khokhar AZ, De La Rue RM, McMeekin SG, Johnson NP (2009) Asymmetric split ring resonators for optical sensing of organic materials. Opt Express 17(2):1107–1115
27. Singh R, Al-Naib IA, Yang Y, Chowdhury DR, Cao W, Rockstuhl C, Ozaki T, Morandotti R, Zhang W (2011) Observing metamaterial induced transparency in individual Fano resonators with broken symmetry. Appl Phys Lett 99(20):201107
28. Johnson PB, Christy R-W (1972) Optical constants of the noble metals. Phys Rev B 6(12):4370

29. Li Z, Ma Y, Huang R, Singh R, Gu J, Tian Z, Han J, Zhang W (2011) Manipulating the plasmon-induced transparency in terahertz metamaterials. Opt Express 19(9):8912–8919
30. Brown LV, Sobhani H, Lassiter JB, Nordlander P, Halas NJ (2010) Heterodimers: plasmonic properties of mismatched nanoparticle pairs. ACS Nano 4(2):819–832
31. Banaee MG, Crozier KB (2010) Mixed dimer double-resonance substrates for surface-enhanced Raman spectroscopy. ACS Nano 5(1):307–314
32. Kim D-S, Heo J, Ahn S-H, Han SW, Yun WS, Kim ZH (2009) Real-space mapping of the strongly coupled plasmons of nanoparticle dimers. Nano Lett 9(10):3619–3625
33. Grillet N, Manchon D, Bertorelle F, Bonnet C, Broyer M, Cottancin E, Lermé J, Hillenkamp M, Pellarin M (2011) Plasmon coupling in silver nanocube dimers: resonance splitting induced by edge rounding. ACS Nano 5(12):9450–9462
34. Liu S-D, Yang Y-B, Chen Z-H, Wang W-J, Fei H-M, Zhang M-J, Wang Y-C (2013) Excitation of multiple Fano resonances in plasmonic clusters with D2h point group symmetry. J Phys Chem C 117(27):14218–14228
35. Hao F, Sonnefraud Y, Dorpe PV, Maier SA, Halas NJ, Nordlander P (2008) Symmetry breaking in plasmonic nanocavities: subradiant LSPR sensing and a tunable Fano resonance. Nano Lett 8(11):3983–3988
36. López-Tejeira F, Rn P-D, Sánchez-Gil JA (2012) High-performance nanosensors based on plasmonic Fano-like Interference: probing refractive index with individual nanorice and nanobelts. ACS Nano 6(10):8989–8996